Application of Diode Laser Molecular Absorption Spectroscopy for Studies of Gas Concentrations in Food Packages

Jan von Keitz

Bachelor Thesis

Spring Semester 2014

Supervisors: Patrik Lundin, Mei Liang and Prof. Sune Svanberg

LUND
UNIVERSITY

Abstract

When it comes to absorbing and emitting radiation, molecules show similar properties as atoms do. A significant difference though, is that a molecular spectrum consists of notably more absorption lines compared to an atomic spectrum. The additional lines appear due to the fact that molecules can not only exist in electronic, but also in vibrational and rotational energy states. Each gas has uniquely defined absorption lines, which makes it possible to associate a fingerprint to the gas. Molecular spectroscopy enables to scan over these lines to determine the existence of a specific gas. With, for example, the help of Tunable Diode Laser Absorption Spectroscopy (TDLAS), which has been used in this work, and by applying the Beer-Lambert law, also the gas concentration can be obtained. Nevertheless, for a precise calculation of the gas concentration the path length travelled by light needs to be available. This especially can cause difficulties when turbid materials are examined, in which the light scatters a lot, and therefore the dimension of the sample does not correspond to the path length of the light anymore.
This work includes the examination of food packages filled with modified atmosphere. Diode lasers emitting wavelengths around 760 nm and 2054 nm are used to scan over an absorption line of oxygen and carbon dioxide, respectively. First, it is presented how the carbon dioxide concentration of 75 % in a sealed bread rolls package is obtained. Afterwards TDLAS combined with a technique called Wavelength Modulation Spectroscopy (WMS), which allows to detect low absorption signals, is used to perform a time dependent measurement on a package with ageing milk inside. The carbon dioxide and oxygen concentrations are monitored simultaneously over 5 days. With the relation between the two concentrations it is possible to speculate about biological activity in the milk package. Another important aspect is, that all the measurements are done non-intrusively, which leaves the package intact allowing usage after the measurement.

List of abbreviations

TDLAS	Tunable Diode Laser Absorption Spectroscopy
WMS	Wavelength Modulation Spectroscopy
GASMAS	Gas in Scattering Media Absorption Spectroscopy
UV	Ultra violet
TEC	Thermo-Electric Cooler
SNR	Signal-to-Noise Ratio
DAQ	Data Acquisition
FDPM	Frequency Domain Photon Migration

Contents

1 Introduction **5**

2 Theory **5**

2.1 Molecular physics 5

2.2 Spectral line broadening 6

2.2.1 Natural broadening 6

2.2.2 Doppler broadening 6

2.2.3 Collision/Pressure broadening 6

2.3 Tunable Diode Laser Absorption Spectroscopy (TDLAS) 7

2.3.1 Diode lasers and photodiodes 7

2.3.2 The principle of TDLAS 7

2.4 The Beer–Lambert law 8

2.5 Wavelength Modulation Spectroscopy (WMS) 9

3 Measurement procedure and experimental setup **10**

3.1 Setup 11

3.2 Head space measurement of bread rolls 12

3.3 Decay process in milk 12

4 Data and analysis **13**

4.1 Data of the head space measurement of bread rolls 13

4.2 Data of the spoiling milk measurement 15

5 Discussion and outlook **17**

6 Self-reflection **19**

7 Acknowledgements **19**

8 References **20**

1 Introduction

The Applied Molecular Spectroscopy and Remote Sensing Group at the Atomic Physics Division, Lund University, has been pursuing studies based on the technique Gas in Scattering Media Absorption Spectroscopy (GASMAS), during the past ten years. The application area is wide, and among other things, examination of gas concentrations in food packaging has been performed. Especially the presence of modified atmospheres in food packages, to extend shelf life and control depravation, is an interesting field of study.
This thesis describes the general application of Tunable Diode Laser Absorption Spectroscopy (TDLAS), combined with Wavelength Modulation Spectroscopy (WMS), in order to examine the carbon dioxide (CO_2) concentration in the head space of food packages. As a specific example the oxygen (O_2) and carbon dioxide concentrations of ageing milk is investigated over time. The experiments performed are used to show the capabilities and limitations of the measurement techniques used. Not only the technique used, but also the data analysis performed are described.
A brief recapitulation of molecular structure and spectroscopy, as well as a description of the most important constituents in the experiments are provided in the next sections.

2 Theory

2.1 Molecular physics

Molecules exist in quantized states with energy E. In comparison to atomic physics the molecule does not only have electronic energy states with energy $E_{\text{el.}}$, but also vibrational states with energy $E_{\text{vib.}}$ and rotational states with energy $E_{\text{rot.}}$. The Born-Oppenheimer approximation allows each energy state to be treated separately. Thus, the total energy E is given by

$$E = E_{\text{el.}} + E_{\text{vib.}} + E_{\text{rot.}}\,. \tag{1}$$

The description of vibrational and rotational states involves new quantum numbers. By considering the selection rules, transitions between different energy levels, E_i and E_j, can take place with absorption or emission of light of a particular frequency. The energy difference $\Delta E = E_i$ - E_j determines the frequency ν of the emitted or absorbed light by

$$|\Delta E| = h \cdot \nu = h \cdot \frac{c}{\lambda}, \tag{2}$$

where h is the Planck constant, c the propagation velocity of the light and λ the wavelength of the light. At this point it is important to consider the energy scales. The electronic transition wavelengths mainly lie in the visible and UV regions, whereas the vibrational and the rotational transitions are mainly situated in the mid-infrared (3–8 μm) and far infrared (30-150 μm), respectively[1]. Because of the large number of energy sub levels, spectra of molecules have considerably more lines compared to atomic spectra.
For a deeper explanation the reader is referred to [2].

2.2 Spectral line broadening

In practice, the light emitted in a transition between energy levels does not have a single particular frequency. It consists of a narrow band of frequencies. The width of this band is called line width. Three main broadening types can describe the line profile, as individually discussed in the following subsections.

2.2.1 Natural broadening

The relation between time and energy described by the Heisenberg uncertainty principle has effects on the line broadening. An excited electronic state with a lifetime τ has an energy uncertainty of $\Delta E \approx h/(2\pi \cdot \tau)$. With $E = h \cdot \nu$ this gives a natural line width of

$$\Delta\nu_{\text{nat.}} \approx \frac{1}{2\pi\tau}. \tag{3}$$

This kind of broadening gives rise to a Lorentzian line shape. The width is of the order of 0.01 Hz for an almost forbidden O_2 transition at 760 nm with a very long upper-state lifetime of 7.1 s.[5]

2.2.2 Doppler broadening

Molecules in a gas are always moving. With an molecular velocity $\bar{\boldsymbol{\nu}}$, the absorption frequency ν_{A} is Doppler-shifted to

$$\nu_{\text{A}} = \nu_0 + \bar{\boldsymbol{\nu}} \cdot \boldsymbol{k}\,, \tag{4}$$

where, $\boldsymbol{k}$, is the wave vector of the light and ν_0, the absorption frequency for a molecule at rest. The statistical spread of the molecular velocities is described by a Maxwell-Boltzmann distribution. The Doppler shift due to the molecular movements results in a Gaussian line shape

$$f_{\text{dop.}}(\nu) = \frac{\sqrt{\ln 2}}{\sqrt{\pi}\Delta\nu_{\text{dop.}}} e^{-\ln 2\left(\nu/\Delta\nu_{\text{dop.}}\right)^2}, \tag{5}$$

with the Doppler line width

$$\Delta\nu_{\text{dop.}} = \nu_0 \frac{2\sqrt{2\ R\ T\ \ln 2}}{c\sqrt{M}}, \tag{6}$$

where T is the temperature, R the general gas constant and M the molecular mass. The width is of the order of around 0.5 GHz[5].

2.2.3 Collision/Pressure broadening

Intermolecular interactions in a gas are reasons for shifting and broadening energy levels of molecules. Shortening of the states lifetime appears and cause broadening. Interactions occur when molecules collide. Therefore the line width gets larger with increasing density and pressure P. The collision line width is given by

$$\Delta\nu_{\text{col.}} = 4\sigma^2 \sqrt{\frac{\pi}{R\ M}} \cdot \frac{P}{\sqrt{T}}\,, \tag{7}$$

where σ is the collisional cross-section. Just like the natural broadening, the collision broadening gives rise to a Lorentzian line shape function

$$f_{\text{col.}}(\nu) = \frac{\Delta\nu_{\text{col.}}}{\pi\left(\left(\nu - \nu_0\right)^2 + \Delta\nu_{\text{col.}}^2\right)}\,. \tag{8}$$

The collision line width is of the order of 1.5 GHz.[5] Recapitulating, one can see that at room temperature and atmospheric pressure, collision broadening has the most dominant effect on the line shape.
A detailed derivation of the line width and line shape for each case can be found in [2].

2.3 Tunable Diode Laser Absorption Spectroscopy (TDLAS)

2.3.1 Diode lasers and photodiodes

To construct a diode laser, p- and n-doped materials are combined. So called holes from the p-doped and free electrons from the n-doped material recombine until an equilibrium between the diffusion potential and the electric potential is reached. A depletion region without free charge carriers is established. By applying a forward current, electrons and holes are constantly injected to the barrier layer. The minority carriers recombine with each other and light can thereby be emitted.
A resonator around the diode amplifies the radiation and laser light is emitted. The semiconductor material defines the band gap of the diode. A material frequently used in the early development is gallium arsenide (GaAs). Most materials used have direct band gaps, which allows an efficient transition. The size of the gap defines the emitted wavelength. Varying the temperature changes the band gap and the index of refraction. Here an increase in temperature provides a longer wavelength. This effect can be used for coarse wavelength tuning, whereas fine tuning over small ranges can be achieved by ramping the current[7]. A higher current creates a smaller band gap which leads to a longer wavelength.
Photodiodes are in principle built up in the same way. The difference here is that incoming photons break up the electron hole pairs and a current is generated and can be measured.

2.3.2 The principle of TDLAS

Tunable diode laser absorption spectroscopy uses the fact that diode lasers emit light with selective wavelengths. The main idea of TDLAS is to examine a characteristic absorption line of a gas spectrum. In order to do so, the temperature of the diode laser is set to a constant value with the help of a Thermo-Electric Cooler (TEC), leading to roughly the needed wavelength. A TEC is a semiconductor based element, which makes use of the Peltier effect. Therefore, the temperature of the laser can be controlled electronically. By applying a ramped current to the diode laser, the wavelength of the emitted light is changing with time.
The light is sent through a sample and the transmitted light is recorded with a suitable detector.

If the temperature and ramping current are chosen properly an absorption profile is obtained. If no line is found, the procedure can be repeated with a different temperature on the diode. A typical absorption profile can be seen in Fig. 6a. The technique has its advantage in examining a particular gas in a mixture. The specific absorption lines are often not influenced by other gases. However, each laser can generally examine only one specific gas due to the limited tuning range.
Sometimes the absorption signal is very small. If that is the case, techniques can be used to improve the Signal-to-Noise Ratio (SNR). One example is the wavelength modulation spectroscopy technique, described in Sec. 2.5.

2.4 The Beer–Lambert law

Light travelling through and absorptive medium decreases in intensity. The exponential decay of the intensity I_0 to I is given by the Beer–Lambert law

$$I = I_0 \cdot e^{-A} = I_0 \cdot e^{-LC\varepsilon(\lambda)}, \tag{9}$$

where the absorbance $A = L \cdot C \cdot \varepsilon(\lambda)$ consists of the path length, L, the concentration, C, and the absorption cross section, $\varepsilon(\lambda)$. The absorption cross section describes the strength of the absorption at a particular wavelength, λ, and the path length expresses the distance travelled by the light through the medium. A measurement with a gas cell with known gas concentration and path length (length of the cell) can provide the absorption cross section by rearranging Eq. 9 in the following way:

$$\varepsilon(\lambda) = \ln\left(\frac{I_0}{I}\right) \cdot (C \cdot L)^{-1} \tag{10}$$

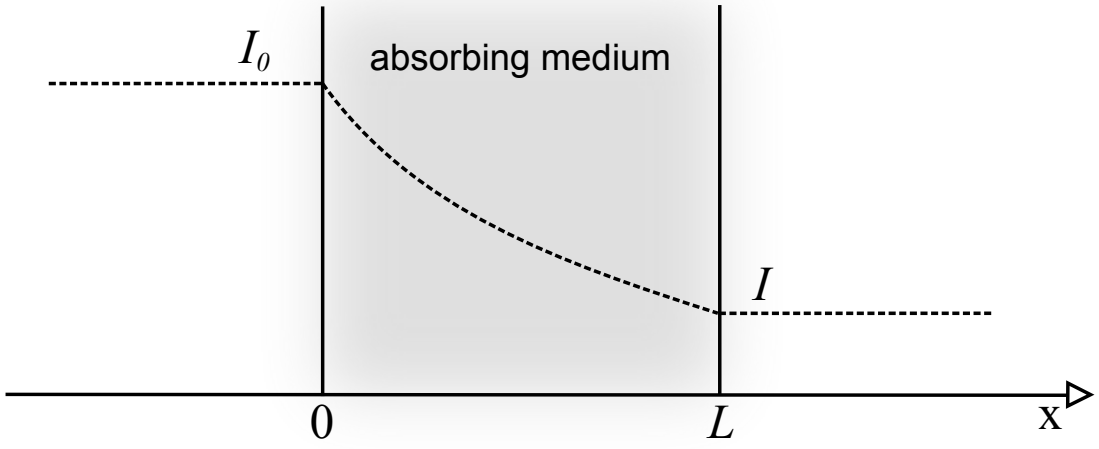

Figure 1: Visualization of the Beer-Lambert law

2.5 Wavelength Modulation Spectroscopy (WMS)

Wavelength Modulation Spectroscopy (WMS) is used to detect low absorption signals. The main limitation for detecting low absorption signals is the signal-to-noise ratio. Flicker noise (or $1/f$ noise) dominates at low frequencies and decreases approximately as $1/f$, where f is the frequency of the signal. The $1/f$ noise has its origin in the electronics of the devices used. Hence, it is obvious that shifting the measurement to a higher frequency will improve the SNR. In the WMS technique the shifting is done by modulating the wavelength in a sinusoidal manner with a modulation frequency f_{m} in the kHz regime. As mentioned in Sec. 2.2.3, the absorption line shape is a non-linear function of the optical frequency (or wavelength). Due to the non-linearity of the line shape and the sinusoidal modulation, the absorption signal will contain higher harmonics which are multiples of the modulation frequency, f_{m}. This is illustrated in Fig. 2.

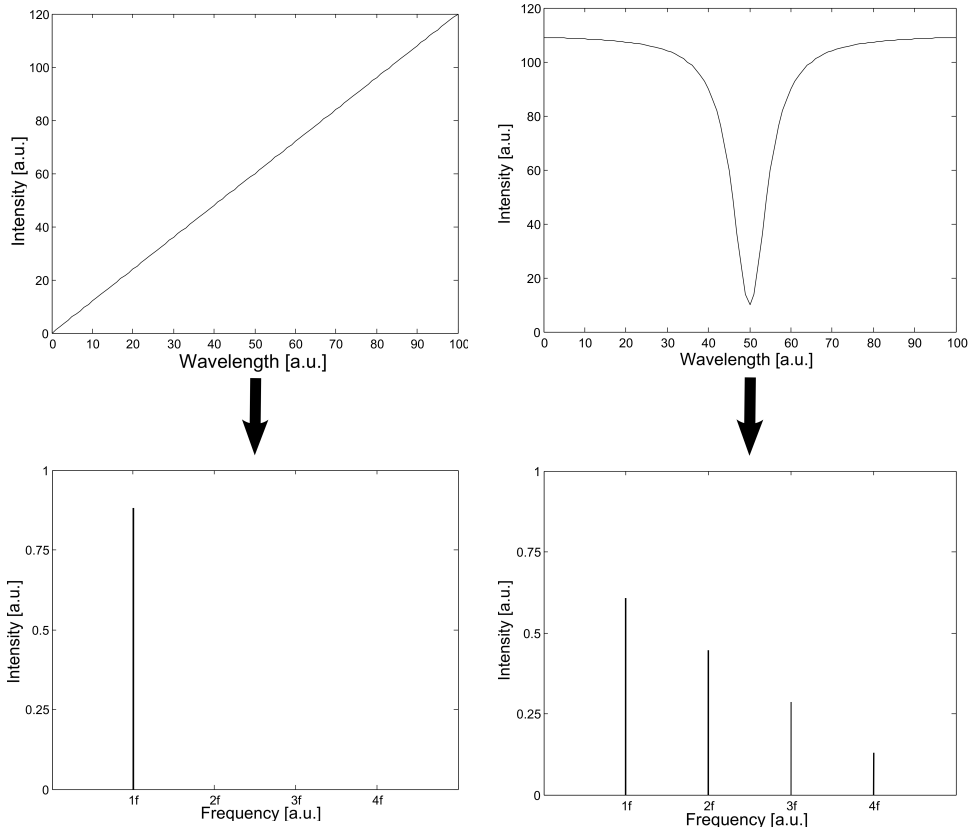

(a) Linear (b) Non-linear

Figure 2: Different relationships between intensity and wavelength and their frequency components. The figure is inspired by [3].

For a linear relationship between intensity and wavelength (Fig. 2a) only the modulation frequency f_{m} gives rise to the frequency spectrum. In contrast, the frequency spectrum of a non-linear relationship between intensity and wavelength (Fig. 2b) contains multiples of f_{m}. The non-linearity in Fig. 2b is represented by a Lorentzian line shape as mentioned in Sec.

2.2.3.

To achieve a sinusoidal modulation, the injection current of the diode laser, which is proportional to the frequency, is managed in the way that

$$\nu(\mathrm{t}) = \nu_0 + \nu_\mathrm{A} \cdot \cos(2\pi f_\mathrm{m} \mathrm{t}), \tag{11}$$

where ν_0 is called the centre frequency and ν_A is the modulation amplitude. The demodulation of the signal, which in principle means filtering out a higher harmonic, can be done in several ways.

A long established method to filter out the higher harmonics is the use of a lock-in amplifier. A lock in amplifier extracts a higher harmonic in the following way. A sinusoidal reference signal $S_\mathrm{ref.}$, with the frequency nf_m and adjustable phase Φ, is multiplied with the detected signal $S_\mathrm{det.}$ and afterwards passed through a low-pass filter. The resulting cross correlation of $S_\mathrm{det.}$, and $S_\mathrm{ref.}$ differs from zero only for matching frequencies. Therefore, with the correct choice of Φ, the nth harmonic is filtered out. Another way is to obtain the harmonics by the use of software based Fourier analysis.

It can be shown that, at small modulation amplitudes, the nth harmonic is proportional to the nth derivative of the line shape function. Additionally, except for the first, the harmonics are proportional to the absorbance, A [4], and therefore also to the concentration C. The first harmonic gives zero at the point of absorption, because the line shape function has an extremum there. Again, this only holds for small ν_A, which means that ν_A should be much smaller than the full width at half maximum of the absorption profile. For higher ν_A this only holds approximately [6]. However, the possibility to obtain a better SNR motivates the use of large modulation amplitudes.

Filtering out the second harmonic ($2f_\mathrm{m}$) has valuable advantages. On the one hand the offset will be zero. This holds because the intensity outside the absorption profile is linear to the current (see e.g. Fig. 6a). Thus, the second derivative vanishes in the linear region. On the other hand it is handy to obtain the peak value of the $2f_\mathrm{m}$ signal which is proportional to the concentration C. Typical $2f_\mathrm{m}$ signals are shown in Fig. 8.

3 Measurement procedure and experimental setup

By analysing the Beer-Lambert law one can see that for a given absorption cross section $\varepsilon(\lambda)$ and a measurement of the intensities I and I_0, there are still two independent variables left; the path length, L, and the concentration, C. As a consequence, the classification of a concentration always involves a measurement of the path length. Measuring the path length can be problematic in highly scattering media. In this case the thickness of the object is not equal to the distance travelled by the light, and it becomes problematic to obtain the true light path length. In a first experiment (Sec. 3.2) the path length is estimated by a simple length measurement of a package with little scattering. In a second experiment (Sec. 3.3) the calibration for concentration determinations is done differently and described explicitly in Sec. 3.3.

3.1 Setup

Fig. 3 illustrates the schematic setup of the experiment. Two different kinds of single-frequency diode lasers are used separately or simultaneously, depending on the experiment. The laser to detect carbon dioxide can be tuned between the wavelengths 2052.5 nm and 2057.5 nm. The laser probing oxygen emits around 760 nm. Constant temperature for the lasers is provided by a TEC.

A Data Acquisition (DAQ) card converts an analog signal to a digital signal and the other way round. On one hand the DAQ card is used to actuate the laser driver. The laser driver is provided with a ramped current to scan the wavelength over the relevant region. Further, the modulation of the signal in the kHz region (9.015 kHz for CO_2 and 10.295 kHz for O_2) for the WMS signal is handled by a computer, connected to the DAQ card. On the other hand the DAQ card is used to provide lock-in detection with the reference signal. $S_{\text{ref.}}$ is created by using a high pass filter to let only the needed higher frequency (nf_{m}) to the lock-in amplifier. In the lock-in amplifier, inputs for $S_{\text{ref.}}$ and $S_{\text{det.}}$ and one output are present. It furthermore consists of a multiplier, a phase shifter for $S_{\text{ref.}}$ and a low pass filter with subsequent integration to create the cross correlation between the two inputs.

Each beam is collimated by a lens. The sample is put between the laser and the detector. For each laser a photodiode is used to detect the signal. Here, the different modulation frequencies for probing of the two gases would allow for the use of a single detector. However, since the wavelengths are so different, a single detector element can usually not detect the light of both lasers efficiently. After amplification the signal is sent to a DAQ card and the lock-in amplifier is used to achieve a WMS measurement. Output and input of the DAQ card are controlled by a LabVIEW program. The costs of a system is depending on the number of lasers that are used. A single laser system costs around 10,000 euros.

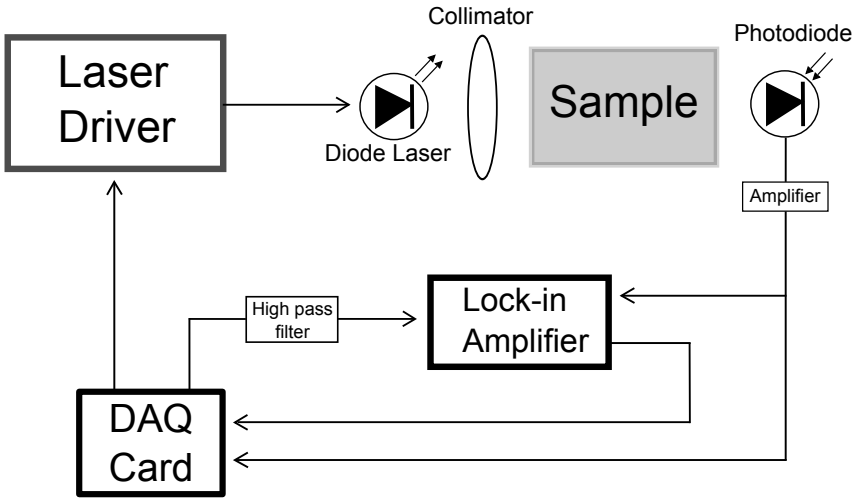

Figure 3: Schematic setup

3.2 Head space measurement of bread rolls

The aim of the first experiment is to obtain the CO_2 concentration in a package of bread rolls. Use of the WMS technique is not needed in this experiment, since the absorption is strong. Therefore the modulation in the kHz region is omitted. At first a calibration measurement on a gas cell with 100 % CO_2 is done. The absorption spectrum is recorded by the photodiode. This enables calculation of the absorption cross section, $\varepsilon(\lambda_{CO_2})$, with Eq. 10. A measurement on the head space of bread rolls is followed. The package was squeezed to get most of the gas into the head space. In this experiment the assumption is made that there is nearly no scattering in the transparent plastic of the package. Therefore, the diameter of the package, simply measured with a caliper, is used as the path length. The data and the analysis are presented in Sec. 4.1. In Fig. 4 a picture of the setup is presented. On the right side of the picture the diode laser can be seen. Directly next to it there is a lens to collimate the beam. On the left side, the detector is set up and in between the laser and the photodiode the bread roll package is placed.

Figure 4: Setup of the bread roll experiment

3.3 Decay process in milk

The aim of the second experiment is to perform a time dependent measurement on an object with varying gas concentration. The object of choice is a package with ageing milk. This time the WMS technique is used to get absorption signals at low concentrations. The emitted light from the lasers detecting CO_2 and O_2 are modulated with modulation frequencies, f_m, of 9015 Hz and 10295 Hz, respectively.

Radiation from the carbon dioxide and oxygen laser is sent through the head space of a milk package which is made out of plastic. This time collimation of the beams is not necessary, because the light gets diffuse when passing the plastic in any case. At first the milk package was

flushed with pure CO_2, to get the peak value of the WMS imprint for 100 % CO_2. Afterwards the CO_2 has been sucked out and the milk package has been left open for 30 minutes to get atmospheric air inside the package. This has been done to make sure that the O_2 concentration was roughly 21 % when the experiment started. The measurement was performed during five days.
The peak values of oxygen at 21 % concentration and carbon dioxide at 100 % concentration are used to calibrate the axes. Hereby it is assumed that the peak value of the $2f_{\mathrm{m}}$ WMS signal scales linearly with the concentration.
The milk package and the fiber of the diode laser to detect the oxygen absorption have been vibrated with a mobile phone vibrator and a small computer fan, respectively. This was done to reduce optical fringes originated from optical interference in the package or fibers.
A presentation of the data and the analysis can be found in Sec. 4.2. In Fig. 5 a picture of the setup is presented. It is similar to Fig. 5. The differences are that no lens is used to collimate the beam, and that this time a second laser and detector (hold by the red clamps) are set up. In addition, the vibrator can also be seen at the holder of the milk package.

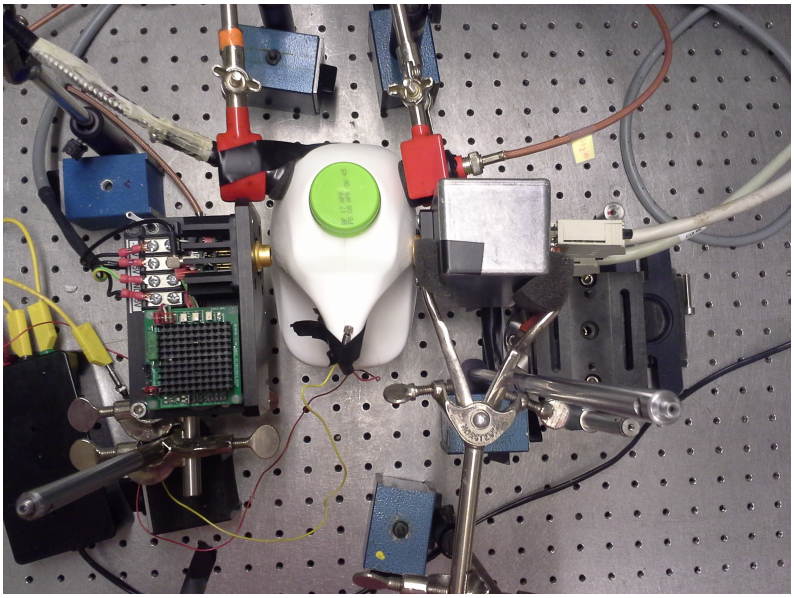

Figure 5: Setup of the milk experiment

4 Data and analysis

4.1 Data of the head space measurement of bread rolls

Figure 6 shows the absorption spectrum of a gas cell with 100 % CO_2. The graphs illustrate the process of the data analysis. Figure 6a shows the scanning over a particular absorption line. This has been done by sawtooth ramping the current of the laser driver. At the stage of no absorption the intensity increases linearly with current (just as the fitted, straight line). A linear least squares fit has been applied. The spectrum is divided by the fitted line, inverted and logarithmised. As mentioned in section 2.2.3, pressure broadening has the largest effect on

the line shape. Therefore, a Lorentzian fit of the line shape function f_p (Eq. 8) is applied. The result is shown in Figure 6b.

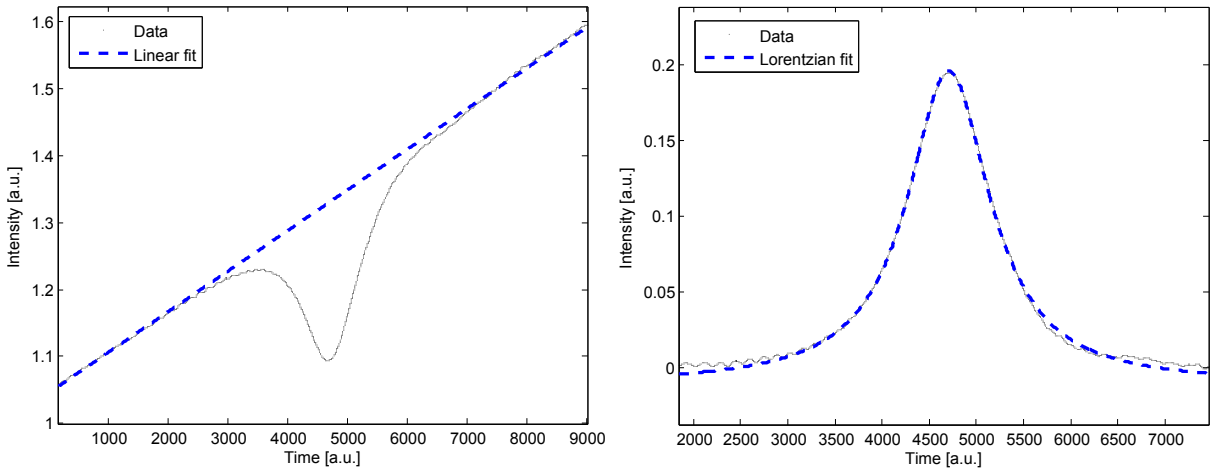

(a) Scanning over the absorption line

(b) Normalized spectrum with Lorentzian fit

Figure 6: CO_2 absorption spectrum of gas cell

The peak value in Fig. 6b corresponds to $\ln\left(\frac{I_0}{I}\right)$. Ten measurements are averaged and give $\ln\left(\frac{I_0}{I}\right)_{av} = 0.197 \pm 0.001$, where the error is the standard deviation. With $L_{cell} = (10.0 \pm 0.1)$ cm and $C = 1$, Eq. 10 gives

$$\varepsilon\left(\lambda_{CO_2}\right) = (0.197 \pm 0.001) \cdot \frac{1}{(10.0 \pm 0.1)\ \text{cm} \cdot 1\ \text{cm}^{-3}} = (0.020 \pm 0.002)\ \text{cm}^2.$$

The value can now be used for other measurements. Of course the laser has to emit at the same wavelength, so that the same absorption line is probed.
The measurements on bread rolls are analysed in the same way. This time $\varepsilon\left(\lambda_{CO_2}\right)$ is given and the concentration C can be calculated with Eq. 10. The length of the package head space is $L_{rolls} = (11.4 \pm 0.1)$ cm. Fig. 7 shows the CO_2 concentration of a bread rolls package. The package has been put into the beam, taken out, and put into the beam again 10 times. This is what the x-axis represents. In each position, the measurement has been done 9 times, successively. This is what the 9 measured points for each position represent. Table 1 outlines the mean concentration (conc.) and standard deviation for each position. In addition the mean value and standard deviation of all points are calculated to

$$C_{\text{bread rolls}} = (77.5 \pm 3.5)\ \%.$$

Table 1: Mean concentration and standard deviation of each position

Position	1	2	3	4	5	6	7	8	9	10
Mean conc. in %	77.81	79.50	77.53	82.40	82.88	79.77	73.64	73.69	78.76	72.54
Standard deviation	0.20	0.08	0.37	0.37	0.52	0.48	0.96	0.11	0.38	0.64

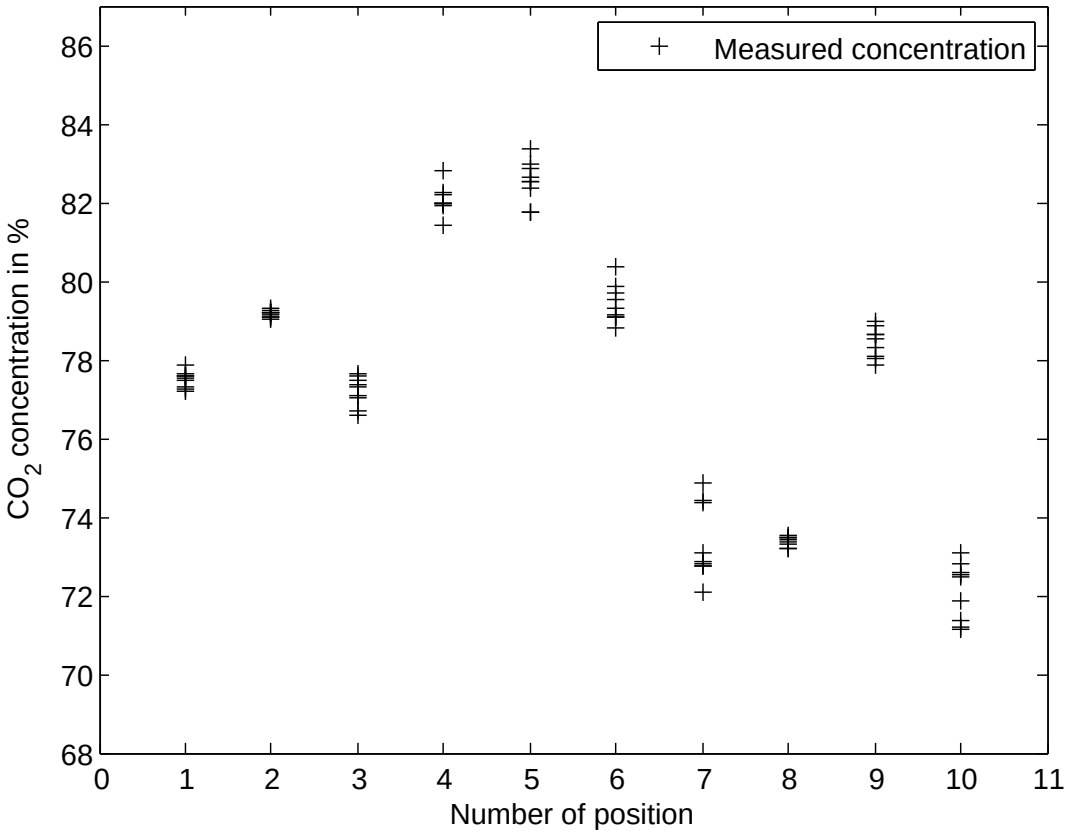

Figure 7: Measurements of CO_2 concentration on a bread rolls package

4.2 Data of the spoiling milk measurement

The CO_2 and oxygen absorption profiles were analysed by a computer program based on Fourier analysis, to obtain the $2f_{\mathrm{m}}$ WMS signal. Typical WMS curves ($2f_{\mathrm{m}}$) for the CO_2 and O_2 absorption are presented in Fig. 8. For each laser, the driver has been ramped with a triangular function. Therefore two peaks are observed, one from increasing current and one from decreasing current. For every absorption signal the two peaks have been averaged. The peak values of the absorption function for the CO_2 absorption at 100 % concentration, and for the oxygen absorption at around 21 % concentration are measured to

$$P_{\mathrm{CO_2}} = 0.0050 \ \text{ and } \ P_{\mathrm{oxygen}} = 0.0015, \tag{12}$$

respectively.

The experiment has been done with a sampling rate of 400 kHz and a buffer (number of data points collected per total triangular ramp) of 80000. Additionally, the values have been averaged 5000 times. This gives a measurement time τ for each triangular ramp of

$$\tau = \frac{80000}{400000 \text{ Hz}} \cdot 5000 = 1000 \text{ s} = 16.67 \text{ min}. \tag{13}$$

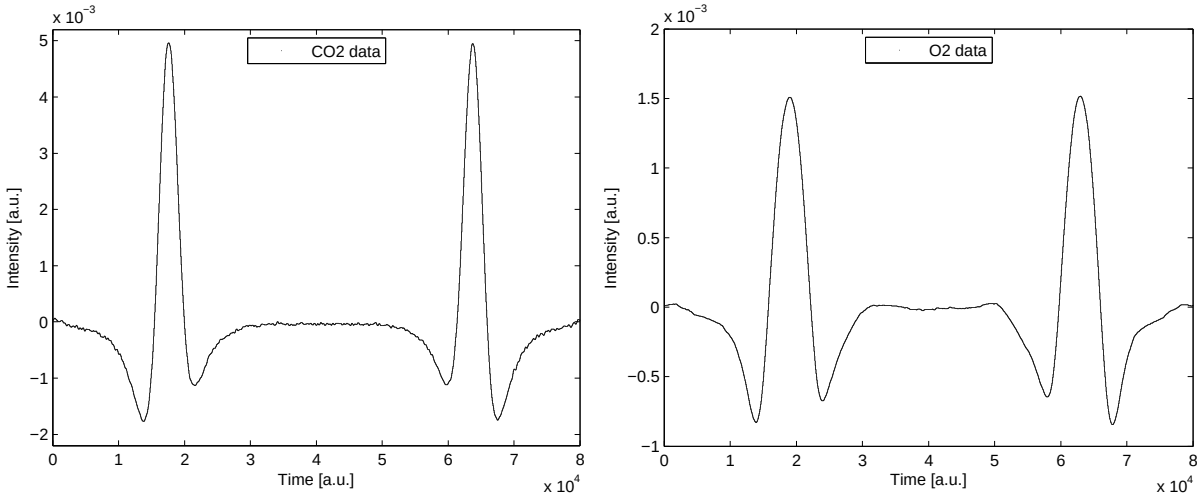

(a) CO_2 absorption at 100 % CO_2 (b) Oxygen absorption at $\approx$ 21 % O_2

Figure 8: WMS absorption profiles ($2f_{\mathrm{m}}$)

In total, 436 measurement points were collected, which gives a total runtime of the experiment of roughly five days. All peak values are presented in Fig. 9. Hereby the y-axis is scaled with the help of $P_{\mathrm{CO_2}}$ and P_{oxygen}, assuming that the concentration scales linearly to zero.

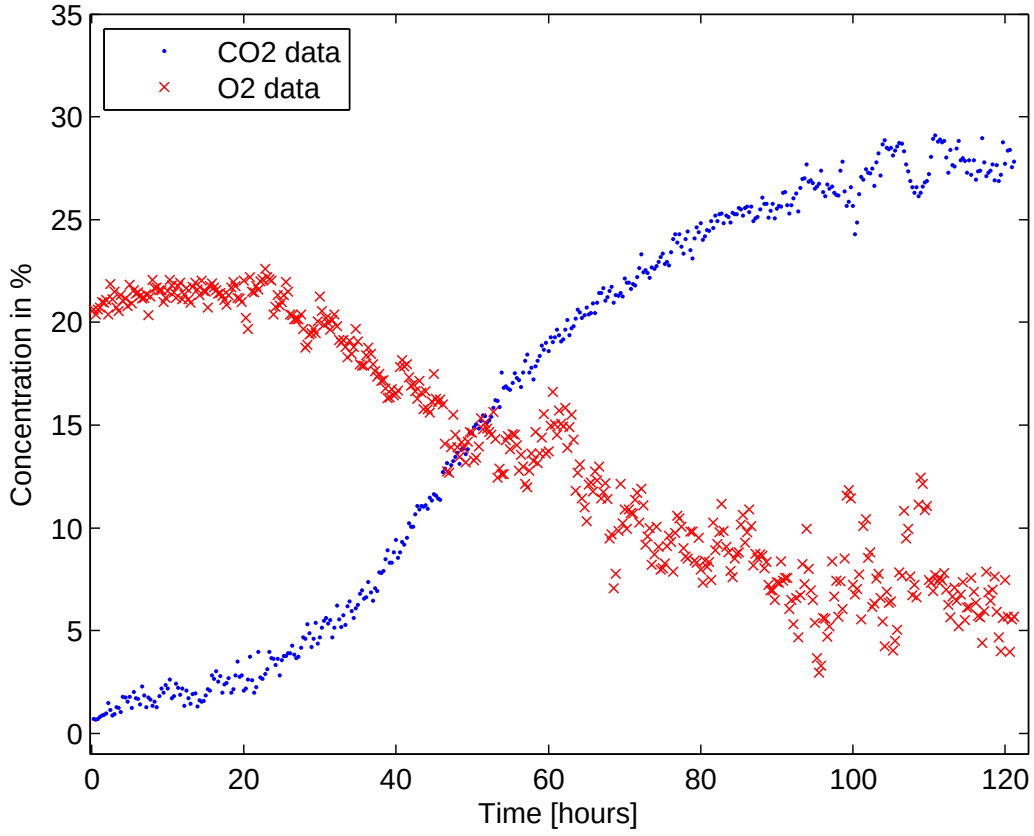

Figure 9: Concentration of CO_2 and Oxygen for spoiling milk

5 Discussion and outlook

At first the results from the bread rolls measurement are discussed. By having a look at Fig. 6b one can see that a Lorentzian fit matches the absorption profile well. This underlines the statement, made in Sec. 2.2.3, that pressure broadening has a dominant effect on the line shape profile at room temperature. The result of measuring the CO_2 concentration inside the package is (77.51 ± 3.47) %. This clearly shows that modified atmosphere has been used in this package. A noticeable high concentration of CO_2 demonstrates that one aim of modifying the atmosphere in food packaging is to diminish the oxygen concentration to reduce the activity of aerobic bacteria. Nevertheless a standard deviation of 3.47 % does not correspond to an accurate measurement. However, by looking at Table 1 the high variation can be explained. The standard deviation of each position is much lower (around 0.35 %). To explain the high deviation of 3.47 %, one has to consider Eq. 9 again which describes the Beer-Lambert law. Only the product of the path length, L, and concentration, C, is proportional to $\ln\left(\frac{I_0}{I}\right)$. The path length in this measurement was assumed to be constant. But by putting the package outside and inside the beam a change in L is unavoidable. Therefore a different L for each position gives a different concentration. Here the problem stated in 3 arises again. The classification of a concentration always involves a measurement of the path length. At the end one can say that a measurement with a known path length would be accurate. Therefore a measurement with the aim to determine a gas concentration should always involve a technique to measure the path length of the traveled light. This especially becomes important in highly scattering media. Several techniques for this purpose are used within our research group. One technique is called Frequency Domain Photon Migration (FDPM). Unfortunately, upgrading the setup with this technique would have gone beyond the work of this bachelor thesis.

Figure 9 presents the time evolution of carbon dioxide and oxygen concentration in a milk package over 5 days. It can clearly be seen that the CO_2 concentration is increasing and the O_2 is decreasing. This can be interpreted as aerobic bacteria consuming oxygen and emitting carbon dioxide. However, it is dubious that the carbon dioxide concentration exceeds that of the initial oxygen concentration. Bacteria should not be able to produce more CO_2 than there was O_2. This can either be explained by a deeper discussion including biological knowledge which is not the purpose of this thesis or by considering that the concentration is only an approximate value (see Sec. 2.5). Another possibility could be that the package was not entirely tight. This would have the effect of a constant oxygen flow into the package, which would allow the bacteria to produce more carbon dioxide.

Besides the discussion of concentrations, an interesting point to mention is the quality loss of the signal after roughly 90 hours. The signal looks more noisy. The reason for this is that the vibrator used to vibrate the milk package broke. Fringes created by interference in the milk package directly influence the measurements quality. Therefore, it has been shown that vibrating objects, with the capability to average out interference patterns, minimize the fringes. All in all it can be said that molecular spectroscopy is a powerful tool for examination of modified

atmosphere in food packaging. Particularly, the combination with WMS gives the ability to also investigate small absorption signals. Certainly, a precise determination of the path length is needed to obtain exact concentration values. An important aspect to keep in mind, is that all the measurements have been done non-intrusively. Other methods which require opening the package implicate unusability after examination. Therefore the technique could for example be used to check food packages directly in a supermarket shelf. This would prevent disposal of expired food which is still eatable.

Another uniqueness is, that the number of gases, which are examined, is only limited by the amount of lasers which can be installed, and possible absorption lines which can be scanned over. Obviously not only O_2 and CO_2 can be investigated. Moreover the milk experiment showed that examination over a period of time can be performed unproblematically. Considering this, the technique might not only be used for examination of food packages but also for studying biological phenomena like bacteria growths and behaviour in specific surroundings. The fact that the WMS technique combined with a technique which determines the lights path length is able to determine gas concentrations for very low absorption signals, also enables to study these phenomena in turbid materials.

6 Self-reflection

When I started my work in the Applied Molecular Spectroscopy and Remote Sensing Research Group my knowledge of diode laser spectroscopy was limited. The only experimental experience in absorption spectroscopy that I had, was given by a basic laboratory exercise about examining fine structure. The work in the group allowed me to set up my own experiment and understand the single parts of the setup. I got a deeper understanding on how to approach a setup and it became clear how long it sometimes can take to get workable data. Furthermore, the dealing with measurement values and their analysis was taught, since it was the first time for me to work with such a large amount of data. Although I had several programming experience before, I learned the handling of Matlab since I never used it before.
Another important point is, that it was the first time for me to experience how it is to work in a research group. It became clear that communication and the ability to express oneself in an understandable way is a key part of successful and effective work.
Nevertheless, the main thing that I have realized is how narrow research areas become. And that in one of these narrow areas, there is still an enormous amount to learn about. One example is that although I got introduced in a theory which is hard to grasp (theory of WMS), I already know that it will take more time to understand it completely.
The last point I want to mention is that the experiment performed revealed the applicability in society or even in other research fields. One example is the control of modified atmosphere. Another one is the milk measurement which lead to an idea to use it for the monitoring of bacterial growth.

7 Acknowledgements

First, I would like to thank Gabriel Somesfalean, who was the first person of the research group that I have talked to. In an one hour meeting he presented the groups current research in every detail. It was very interesting and therefore I want to thank Sune Svanberg for making it possible to participate in the group as a bachelor student. I also want to thank Sune for constantly giving me feedback on my work and having an open mind for every kind of question. I also want to thank Patrik Lundin for taking the time for being my supervisor. You did an excellent job in guiding me through my project and you always had time to answer all my questions. Mei Liang - I also want to thank you for helping me with setting up the experiment and answering all my questions regarding to the laboratory. And of course many thanks to Jim Larsson who introduced me to the subject, helped me with the experiments and especially because he assisted me in doing the data analysis.

8 References

[1] C. N. Banwell and E. M. McCash. *Fundamentals of molecular spectroscopy.* McGraw-Hill Publishing Company, fourth edition, 1994.

[2] W. Demtröder. *Atoms, Molecules and Photons.* Springer Heidelberg, 2006.

[3] P. Kluczynski. *Wavelength modulation spectrometry : a new description of its fundamental principles and properties.* University, Umeå, 2002.

[4] P. Kluczynski, J. Gustafsson, Å. M. Lindberg, and O. Axner. Wavelength modulation absorption spectrometry — an extensive scrutiny of the generation of signals. *Spectrochimica Acta Part B: Atomic Spectroscopy*, 56(8):1277 – 1354, 2001.

[5] M. Lewander. *Laser Absorption Spectroscopy of Gas in Scattering Media.* PhD thesis, Lund Reports on Atomic Physics, LRAP 424, Lund University, 2010.

[6] P. Lundin. *Laser Sensing for Quality Control and Classification – Applications for the Food Industry, Ecology and Medicine.* PhD thesis, Lund Reports on Atomic Physics, LRAP 488, Lund University, 2014.

[7] S. Svanberg. *Atomic and Molecular Spectroscopy.* Fourth edition, Springer Heidelberg, 2004.